International Journal of NanoScience and Nanotechnology
ISSN 0974-3081 Volume 17, Number 1 (2026), pp. 83-92

https://www.ripublication.com

Effect of Li ion on Electronic and Physical Properties of $LiTlSO_4$ over Tl_2SO_4

Rama Rao Samudrala[1,2], Bheema Lingam Chittari[*3], Rajesh Desapogu[3],Vijayalakshmi Raguru Pandu[1], Sunandana Channappayya Shamanna[3]

[1]Department of Physics, College of Sciences, Sri Venkateswara University, Tirupati. [2]Govt. Polytechnic, Department of Technical Education, Nellore, INDIA. [3]School of Physics, University of Hyderabad, Hyderabad, Telangana, INDIA.

*Corresponding author E-mail: *ramarao.samudrala@gmail.com*

Abstract

We report the effect of Li ion presence on electronic and physical properties of $LiTlSO_4$ over Tl_2SO_4. It is revealed that $LiTlSO_4$ has orthorhombic structure similar to Tl_2SO_4. The Li ion addition in Tl_2SO_4 replaces one of the Tl ions. It is found due to the size mismatch of Li & Tl there is a huge volume reduction in $LiTlSO_4$ over Tl_2SO_4 and these results are confirmed with the density functional theory calculations. The computed density of states clearly shows the wide band gaps of 3.78 and 4.17 eV for Tl_2SO_4 and $LiTlSO_4$, respectively. It is also found that due to the presence of Li ions leads to stiffness in the $LiTlSO_4$, which is confirmed from the blue shift in Raman modes. The molecular structure features and different vibrational modes of Tl_2SO_4 and $LiTlSO_4$ have been explored by infrared spectra. It has been revealed that $LiTlSO_4$ has endothermic peaks at 468 and 490.5^0C. In contrast, Tl_2SO_4 has only one endothermic peak at 498^0C. The presence of Li in Tl_2SO_4 has a significant effect on physical properties and it is less pronounced in the case of electronic properties.

Keywords: Ionic compounds; Sulfides; vibrational spectroscopy; Bonding; Ab initio;

1. Introduction

The mechanism of ionic conductivity in the various compositions of mixed alkali metasulphates is completely depends on its structure and arrangement of sub-lattice ions [1-7]. Recently, the various physical and electronic properties of similar sulphites have been explored extensively [8-10]. The alkali metal sulphates (Li_2SO_4, Na_2SO_4, K_2SO_4,Rb_2SO_4 and Cs_2SO_4) are attractive due to their single or successive reversible

structural phase transitions for piezoelectric properties and high ionic conductivity along with the double salts of $MLiSO_4$ (M = Na, K, Rb and Cs) [11]. The sliver and thallous based sulphate crystals are also attracted due to the distinct conductivity of Ag+ and Tl+ [12-16]. The conductivity Ag+ and Tl+ is related to the polarizability which is linked to valence electrons [12-16]. The mixed sulphates like $AgLiSO_4$, $NaLiSO_4$, $RbAgSO_4$,$KLiSO_4$ and $TlAgSO_4$ with two monovalent cations are known to be good solid electrolytes [13]. The understanding of structural difference and chemical change in Tl (or Ag) based sulphate when they mix with the alkali metal atom are interesting to design new class of compounds. Among many, thallous sulphates have drawn a special interest.The layers of thallium sulphides find applications in photonconductive devices and solar batteries due to their variety of stoichiometry and physical properties. Thethallous based sulphites are basically determined by their different (+1 and +3) oxidation states. These thallous sulphides (Tl_2SO_4) have K_2SO_4 structure. The room temperature phase of Tl_2SO_4 (II) has an orthorhombic structure and it transforms to Tl_2SO_4 (I) at 765± 4 K [14]. The mixing of Li with the Tl_2SO_4 forms $LiTlSO_4$ which exists in two crystallographic forms. The low-temperature beta $LiTlSO_4$ is orthorhombic [14] and at high-temperature it forms the alpha phase which is hexagonal symmetry [12]. The effect of Li ion in the presence of Tl on physical and electronic properties of

2. Synthesis and Characterization

The starting material Tl_2SO_4 (ALDRICH) has been taken and used the $Li_2SO_4.H_2O$ (Alfa) and mixed in 1:1 ratio and grinded for one hour in a agate mortor to obtain the $LiTlSO_4$ samples. The obtained powder of $LiTlSO_4$ is heated at 200^0C for 10 hours and subsequently cooled to room temperature. The as prepared samples of $LiTlSO_4$ are again thoroughly grinded and used for further characterization. The crystal structure of the $LiTlSO_4$ sample and Tl_2SO_4 are determined by X-ray powder diffractometer (XRD)using Co Kα radiation (λ = 1.7889 Å).

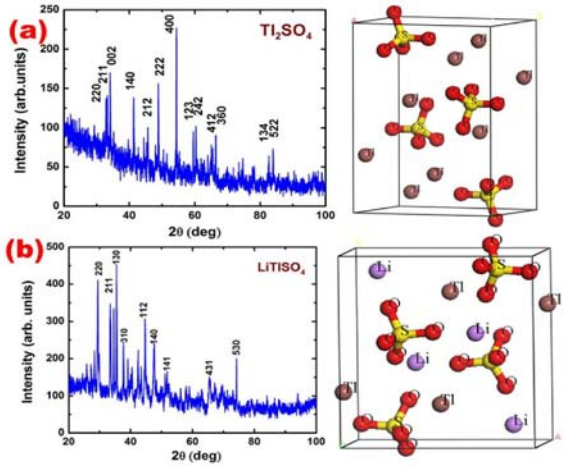

Figure 1. The X-ray diffraction and optimized crystal structure of (a) Tl_2SO_4 and, (b) $LiTlSO_4$.

The morphologies and chemical composition of these samples were obtained from Field emission scanning microscopy (FESEM) and energy dispersive X- ray scattering (EDS) (a model no ULTRA- 55, ZEISS, Japan), respectively. Later, Raman spectra is recorded at 300 K in a back scattering geometry with Horiba Jobin Yvon, LabRAM- HR800 micro-Raman system using 514.5nm excitation from Ar+ gas laser. The endothermic phase transitions are obtained using differential scanning calorimetry (DSC) by DuPont 9900 model DSC instrument.The electron spin resonance spectra (ESR) is used to find the impurity species which is recorded on a JEOL9FE-3X) x-Band spectrometer under optimized conditions of modulation amplitude, receiver gain, time constant and scan time.

3. Theoretical Methods

Besides, we have also calculated the structural and bonding nature of these Tl_2SO_4 and $LiTlSO_4$ compounds by first principles calculations using density functional theory as implemented in the Cambridge Sequential Total Energy Package (CASTEP) [17]. The structure and electronic properties are compared to trace the effect of Li ion presence in Tl_2SO_4. For Tl_2SO_4 and $LiTlSO_4$, the basis orbitals used as valence states are Tl: $5d^{10}$, $6s^2$; S: $4s^2$, $4p^3$; O: $2s^2$; $2p^4$ and Li: $2s^1$. We have used Vanderbilt-type [18] ultrasoft pseudopotentials for the electron–nuclei interactions together with the generalized gradient approximation (GGA) and local density approximation (LDA) for exchange - correlation functionals for electron–electron interactions [19]. A plane wave basis set with an energy cut-off of 400 eV has been used. For the Brillouin zone sampling, a 4 x 7 x 4 Monkhorst–Pack mesh [20] has been used for both the systems, in which the forces on the atoms are converged to less than 0.0005 eV/Å. The maximum ionic displacement is within 0.005Å and the total stress tensor is reduced to the order of 0.02 GPa.

Figure 2. The FE-SEM and EDS of Tl_2SO_4 (a & c) and $LiTlSO_4$(b & d).

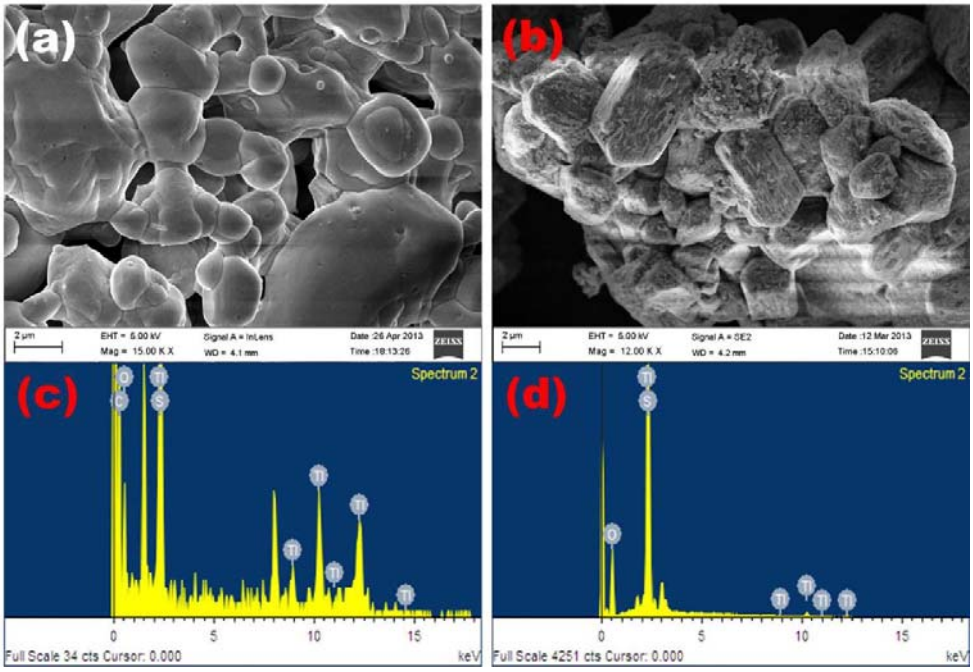

4. Results and Dicussion

4.1. Structure and morphology

The structure and morphology of Tl_2SO_4 and the synthesized $LiTlSO_4$ are obtained from XRD and FESEM. The obtained XRD pattern and the crystal structures of Tl_2SO_4 and $LiTlSO_4$ are shown in Fig.1. From XRD analysis it is identified that $LiTlSO_4$ forms a crystalline phase of orthorhombic structure with the space group of Pnam (62), similar to Tl_2SO_4. The XRD of $LiTlSO_4$ shows peaks at 29.5, 33.5, 35.4, 37.7, 40.6, 47.8, 51.8, 65.5, 74.3 angles of reflections corresponding to the planes (200), (211), (130), (310),(112), (140), (141), (431), and (530) which are in well agreement with the JCPDS 74-1618. We have also compared the peaks for Tl_2SO_4 at 32.9, 33.2, 34, 41.3, 45.7, 48.7, 54.2, 59.5, 60.4, 66.4, 74.8, 28.6, 83.9 angles of corresponding reflections from the planes (220), (211), (002), (140), (212), (222), (400), (123), (242), (412), (360) and (522) which are matching with JCPDS card no's: 52-1592, as shown in Fig 1 (a & b). These results are in well agreement with the previous experiments [12]. For detailed understanding of the structural modification of Tl_2SO_4 after addition of Li, we have considered density functional theory calculations using CASTEP [17]. We adopted the crystal structures from the experiments and fully optimized within generalized gradient approximations (GGA), the obtained structural details such as lattice parameters, atomic positions and volume are summarized in Table.1 & 2 along with experimental data. The optimized crystal structure of Tl_2SO_4 and $LiTlSO_4$ has shown in Fig.1a & b. There is a large reduction along c-axis and expansion along b-axis, similarly a slight expansion in the a-axis in $LiTlSO_4$ compared to Tl_2SO_4. The lattice parameters of Tl_2SO_4 is found to be larger compared to the $LiTlSO_4$, and the total volume is found to be reduced in$LiTlSO_4$ compared to Tl_2SO_4. The Li ion addition in the Tl_2SO_4 replaces on of the Tl,which is subsequently leads to the huge volume reduction due to the mismatch of the sizes of Li and Tl.

Table.1: The optimised lattice parameters along with experimental values of Tl_2SO_4 and $LiTlSO_4$

	Tl_2SO_4		**$LiTlSO_4$**	
Parameters	**LDA (GGA)**	**Expt (Ref.12)**	**LDA (GGA)**	**Expt (Ref.12)**
a (Å)	7.654 (8.060)	7.818	8.408 (8.893)	8.388
b (Å)	5.737 (5.944)	5.931	8.902 (9.348)	9.309
c (Å)	10.49 (11.67)	10.63	5.187 (5.387)	5.328
V(Å^3)	460.8 (559.5)	493.0	388.3 (447.9)	416.0

Table.2:The atomic coordinates of Tl_2SO_4 and $LiTlSO_4$

		Tl_2SO_4			$LiTlSO_4$	
Atoms	x/a	y/b	z/c	x/a	y/b	z/c
Tl (1)	0.669	0.250	0.432	0.495	0.218	0.745
Tl (2)/Li	0.992	0.250	0.695	0.322	0.412	0.245
S	0.211	0.250	0.427	0.207	0.079	0.245
O (1)	0.279	0.042	0.370	0.041	0.093	0.250
O (2)	0.026	0.250	0.421	0.275	0.214	0.149
O (3)	0.267	0.250	0.551	0.264	0.050	0.502
O (4)	-	-	-	0.252	-0.042	0.079

The average lattice parameters error percentage of LDA and GGA with the experiments in the case of $LiTlSO_4$ is found to be about 3% on other hand Tl_2SO_4 show 3% with LDA and 5% with GGA. In particular a-, b- and c-axis in Tl_2SO_4 and $LiTlSO_4$ have 2% (3%), 3% (0.2%) & 1% (9%) and 0.2% (6%), 4% (0.4%) & 2% (1%) error with LDA (GGA), respectively. The variations in the error along different directions are due to the interactions variation. The notable variation in b- & c-axis in Tl_2SO_4 and a- & b-axis in $LiTlSO_4$ is may be because of long range interactions between Tl (and/or Li) and SO_4.The morphology and surface characteristics are investigated through FESEM as shown in Fig.2a & b for Tl_2SO_4 and $LiTlSO_4$. These samples show micro sized particle with average size of ~8-12µm. It is found that Tl_2SO_4 has ductile surface whereas $LiTlSO_4$ has brittle surface, which is because of the Li presence leads to stiffness in the $LiTlSO_4$. The elemental analysis of Tl_2SO_4 and $LiTlSO_4$ samples are determined by using EDS technique as shown in Fig. 2c & d. The EDS clearly shows the compound formation from Tl, O and S elements and confirms the chemical composition of Tl_2SO_4 and $LiTlSO_4$ with almost in stoichiometric ratios.

4.2. Density of states and Charge density

The Li addition in the Tl_2SO_4 brought a significant reduction in the volume, which is

defiantly effects the entire interactions and chemical structure. Here, we have explored the electronic structure and bonding properties of Tl_2SO_4 and $LiTlSO_4$ from density of states and charge density distribution. The calculated total density of states is shown in Fig.3a & b for Tl_2SO_4 and $LiTlSO_4$, respectively. The computed density of states clearly shows a wide band gaps between the valance band and conduction bands of Tl_2SO_4 and $LiTlSO_4$. The valence band and the conduction band are both well separated in both the compounds with the values of 3.78 and 4.17 eV for Tl_2SO_4 and $LiTlSO_4$, respectively.From the density of states it is also clear that, the top of the valance band is mainly from the O-2p states of SO_4 group where the bottom of the conduction band is from Tl-p states in both the cases, interestingly there is almost zero contribution from Li. In both the compounds the signatures of the density of states are similar which indicates the negligible difference in the electronic structure by doping Li in Tl_2SO_4. The presence of Li ions in $LiTlSO_4$, over the Tl_2SO_4 enhanced the band gap indicates that the $LiTlSO_4$ is bad electronic conductor compared to Tl_2SO_4. The nature of electronic states near Fermi level is crucial for the effectiveness of charge transfer in a battery and its capacity [5].

The discontinuity in the density of states of both the compounds relate to the localized electronic states, which constitute a kinetic barrier for ions and electrons ambipolar diffusion. In the valance band, the bands around -9 eV are from Tl-5d states, the bands from -6 eV to -5 eV are due to mixture of O-2p & O-2s and S-4p, and the bands from -4 eV to -3 eV are basically due to Tl-6s and -3 eV to -2 eV are from O-2p states alone.The states between -2 to -1 eV are admixture of Tl-6s and O-2p. The Fermi level, O-2p states has a sharp peak indicating predominant behaviour of oxygen in Tl based sulphates.

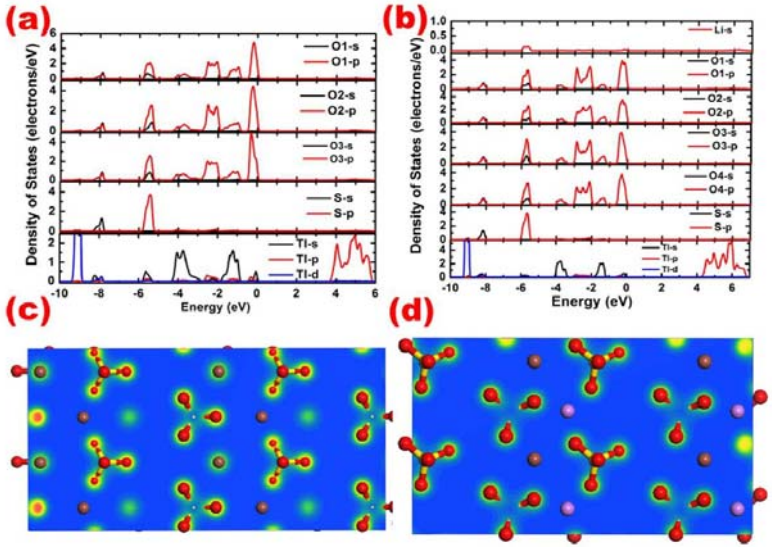

Figure 3. The calculated density of states (a & b) and charge density distribution (c & d) along (100) plane of Tl_2SO_4 and $LiTlSO_4$

The conduction bands are mainly derived from the Tl-p states.Further, we have also investigated the charge density distributions in Tl_2SO_4 and $LiTlSO_4$ in (100) plane as shown in Fig.3c & d, respectively. The non-spherical charge distribution around the oxygen and sulphar atoms indicates the sharing of charge which is the behaviour of covalent nature. The localized charge around Tl and Li atoms is the behaviour of ionic nature. The S-O bonds are covalent in character and separated from the Tl (and Li) in ionic sub-lattice. However, we will show in the following, an analysis of physical properties which reveals that the Li presence brings about a significant change in physical properties of $LiTlSO_4$ over Tl_2SO_4.

4.3. Raman and FTIR spectroscopy

As, we have seen that there is a very slight variation in the electronic and bonding properties upon addition of Li in Tl_2SO_4. Moreover, the Li ion replaces one of the Tl ions in $LiTlSO_4$ there could be a significant effect in the physical properties. Here, we conducted Raman spectroscopic studies for both the $LiTlSO_4$ and Tl_2SO_4. The Raman spectra of synthesized $LiTlSO_4$ along with Tl_2SO_4 powders are recorded by a micro- Raman spectrometer with argon ion laser (514 nm) as the excitation source. The light was focussed on the sample through 100x optical microscope objective in a back scattering geometry. The scattered light was collected by a grating and the entire spectrum was recorded by CCD. The obtained Raman spectra of $LiTlSO_4$ and Tl_2SO_4 are shown in Fig.4a. The Raman spectra of Tl_2SO_4 and $LiTlSO_4$ exhibit six fundamental bands (are ν_{ext}, $\nu1$, $\nu2$, $\nu3$ and $\nu4$) as shown in Fig.4a. The ν_{ext} occurs at 80.5 and 95 cm^{-1}. The intense peak at 998.6 cm^{-1} is denoted as $\nu1$, whereas 462.8 cm^{-1} is under $\nu2$ band.

The peaks near the intense peak 1095 and 1188 cm^{-1} are $\nu3$ band. The $\nu4$ consists of 634.8 cm^{-1}. The bands $\nu1$and $\nu4$ are basically arise from SO_4 group. In $LiTlSO_4$ the bands $\nu1$, $\nu2$ and $\nu4$ are found to shift towards high frequencies compared to Tl_2SO_4.The increase in frequency i.e, blue shift in Raman modes indicates the improved stiffness in the crystal $LiTlSO_4$ over Tl_2SO_4.

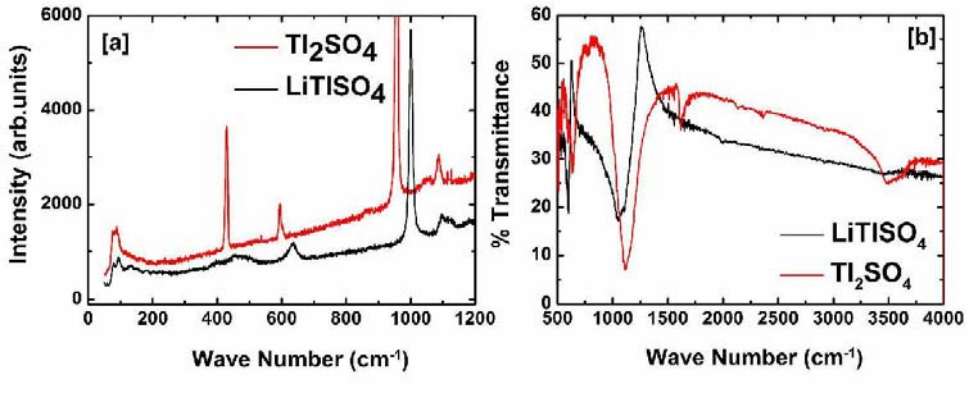

Figure 4. (a) Raman and (b) FTIR spectroscopy of Tl_2SO_4 and $LiTlSO_4$

The molecular structure features and different vibrational modes of Tl_2SO_4 and $LiTlSO_4$ have been explored by FTIR. The infrared (IR) spectrum of $LiTlSO_4$ was recorded in range of 4000 to 500 cm^{-1} using FTIR spectrometer, as shown in Fig.4b. The IR spectrum shows the vibrations at 1114.33, 636.42 and 509.14 cm^{-1} in Tl_2SO_4 whereas 1054.92 and 597.85 cm^{-1} in $LiTlSO_4$ are coupled with sulphate (SO_4) group. The peak at 1997.99 cm^{-1} shows the presence of the both Lithium and Thallium complexes in $LiTlSO_4$. It is well known that while the IR band positions are functions of atomic masses, the band widths are related to charge density fluctuations inside the bond region of Li-O, Tl-O and S-O bonds. The increase in band widths of SO_4^{2-} molecular group of $LiTlSO_4$ indicates that the electronic charge density inside the bond region is being influenced by the mobility of Li+ cations which are surrounding the SO_4^{2-} molecular groups.

4.4. Electron Spin Resonance (ESR) and Differential Scanning Calorimetry (DSC)

Electron spin resonance is a specific microscopic probe with which to examine molecular environments in crystalline and disordered systems. Under favourable circumstances, it is possible to create and stabilize paramagnetic radicals which may reflect certain aspects of structure and dynamics and may be characteristic of the system itself. Presently we describe our efforts to stabilize and identify molecular paramagnetic radicles in Tl_2SO_4 and $LiTlSO_4$. The ESR spectra for $LiTlSO_4$ and Tl_2SO_4 are shown in Fig.5a. Appearance of similar ESR signals for both $LiTlSO_4$ and Tl_2SO_4 suggests a common origin for the paramagnetic centres are involved. The ESR spectrum shows the characteristic six line hyperfine splitting spectrum centred at g = 2.32 for $LiTlSO_4$. The average spacing between the peaks ~9.8 G, g_{av} = 2.07 at a field 329G are observed.

This is due to Mn^{2+} ions in an environment close to octahedral symmetry. The anisotropy in the g-factor in $LiTlSO_4$ is attributed to the coupling of orbital angular momentum to the spin angular momentu$_m$ via spin-orbit coupling. In the case of Tl_2SO_4 the g value is found to be 2.01. As we discussed elsewhere [21] the value of g_{av} greater than 2.0036 is referred to as a 'hole centre' otherwise it is called as 'electron-excess centre'.

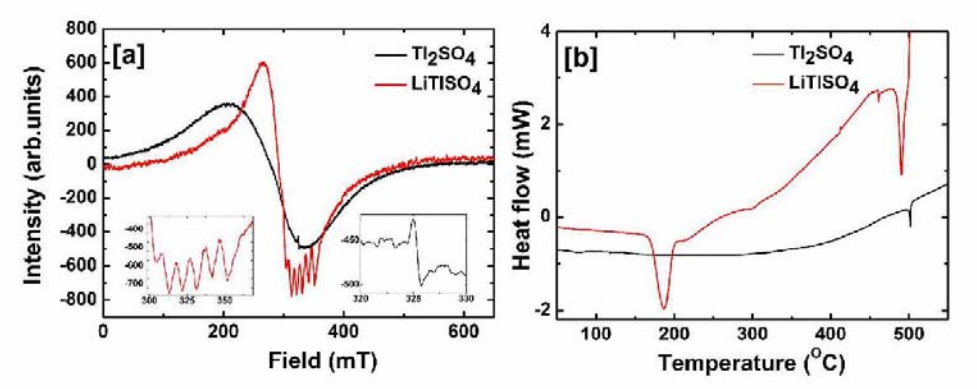

Figure 5. (a) ESR and (b) DSC of Tl_2SO_4 and $LiTlSO_4$.

In both the cases of Tl_2SO_4 and $TlLiSO_4$ the g_{av} value is found to be slightly greater than 2.0036 and known to be 'hole-centre'. The endothermic phase transitions in $LiTlSO_4$ and Tl_2SO_4 have identified from DSC. The DSC curves of Tl_2SO_4 and $LiTlSO_4$ are shown in Fig.5b reveals that $LiTlSO_4$ has endothermic peaks at 468 and 490.5^0C. We suspect that these two endotherms could be due to the inhomogeneous mixing of $LiTlSO_4$. In contrast, Tl_2SO_4 has only one endothermic peak at 498^0C. It was found that the anomaly depend on the turning temperature at which a cooling run was changed to a heating run [4].

5. Conclusion

The $LiTlSO_4$ is synthesised by grinding the $Li_2SO_4.H_2O$ and Tl_2SO_4. The electronic and physical properties of $LiTlSO_4$ have been compared with the Tl_2SO_4. The XRD analysis reveals that LiTlSO4 has orthorhombic structure similar to Tl_2SO_4. The Li

ion is replaced the Tl ions in Tl_2SO_4 resulting in huge volume reduction, these results are confirmed with the density functional theory calculations. The computed density of states clearly shows wide band gaps of 3.78 and 4.17 eV between the valance band and conduction bands of Tl_2SO_4 and $LiTlSO_4$, respectively. The electronic properties are found to have no significant effect upon addition of Li to Tl_2SO_4. In contrast there are significant effects observed in physical properties. It is found that Tl_2SO_4 has ductile surface whereas $LiTlSO_4$ has brittle surface this is due to the presence of Li ions leads to stiffness in the $LiTlSO_4$, which is confirmed from the Raman spectra shift. The molecular structural features and different vibrational modes of Tl_2SO_4 and $LiTlSO_4$ have been explored by FTIR. The IR spectrum shows the vibrations at 1114.33, 636.42 and 509.14 cm^{-1} in Tl_2SO_4 whereas 1054.92 and 597.85 cm^{-1} in $LiTlSO_4$ are coupled with sulphate (SO_4) group. The peak at 1997.99 cm^{-1} shows the presence of the both Lithium and Thallium complexes in $LiTlSO_4$. The ESR spectrum shows the characteristic six line hyperfine splitting spectrum centred at g = 2.32 for $LiTlSO_4$. The average spacing between the peaks ~9.8 G, g_{av} = 2.07 at a field 329G are observed.This is due to Mn^{2+} ions in an environment close to octahedral symmetry. In the case of Tl_2SO_4 the g value is found to be 2.01. From the DSC, it has been revealed that $LiTlSO_4$ has endothermic peaks at 468 and 490.5^0C. In contrast, Tl_2SO_4 has only one endothermic peak at 498^0C. The presence of Li in Tl_2SO_4 there is a significant effect on physical properties and it is less pronounced in the case of electronic properties.

Acknowledgments

Dr. SRR thanks to The Special Commissioner of Technical Education, Amaravathi.

References

[1] L. Zengcai, F. Wujun, E. A. Payzant, Y. Xiang, W. Zili, J. D. Nancy, K. Jim, H. Kunlun, J. R. Adam and L. Chengdu, J. Am. Chem. Soc. 135 (2013) p.975.
[2] Z. Yusheng and D. L. Luke, J. Am. Chem. Soc. 134 (2012) p.15042.
[3] K. Hisashi, O. Kazushige and K. Kunihito, Inorg. Chem. 51 (2012) p.9259.
[4] A. N. Radhakrishnan, P. Prabhakar Rao, S. K. Mahesh, D. S. Vaisakhan Thampi and K. Peter, Inorg. Chem. 51 (2012) p.2409.
[5] J. Molenda, Funct. Mater. Lett. 4 (2011) p.107.
[6] Z. Xin-Xing and L. Min, J. Phys. Chem. Lett. 4 (2013) p.1205.
[7] R. A. Secco and E. A. Secco, J. Phys. Chem. Solids. 56 (1995) p.1045.
[8] S. Rama Rao, Ch. Bheema Lingam, D. Rajesh, R. P. Vijayalakshmi and C. S. Sunandana, Eur. Phys. J. App. Phys. 66 (2014) p.30906.
[9] S. Rama Rao, Ch. Bheema Lingam, D. Rajesh, R. P. Vijayalakshmi and C. S. Sunandana, Int. J. Nanosci. Nanotech. 4 (2013) p.201.
[10] S. Rama Rao, Ch. Bheema Lingam, D. Rajesh, R. P. Vijayalakshmi and C. S. Sunandana, IOSR. J. App. Phys. 4 (2013) p.39.
[11] K. Singh and S. S. Bhoga, Bull. Electrochem, 12 (1996) p.633.
[12] H. Kasano, S. Tsuchiyama, Y. Kawamura and H. Mashiyama, Ferroelectrics, 217 (1998) p.121.
[13] H. Mashiyama, J. Wu, F. Shimizu and M. Takashige, J. Phys. Soc. Jap. 67 (1998) p.359.
[14] S. Rama Rao and C. S. Sunandana, Solid. State. Commun, 98 (1996) p.927.
[15] Y. Lu and E. A. Secco, Solid State Ionics, 53-56 (1992) p.223.
[16] A. Elfakir, J. Souron, G. Wallez, M. Quarton and M.Touboul, Solid State Ionics, 110 (1998) 145.
[17] M. Segall, P. Lindan, M. Probert, C. Pickard, P. Hasnip, S. Clark, M. Payne, J. Phys.: Condens. Matter. 14 (2002) p.2717.
[18] D. Vanderbilt, Phys. Rev. B. 41 (1990) p.7892.
[19] J. P. Perdew, K. Burke, M. Ernzerhof, Phys. Rev. Lett. 77 (1996) p.3865.
[20] H. J. Monkhorst, J. Pack, Phys. Rev. B. 13 (1976) p.5188.
[21] C. S. Sunandana, Bull. Mater. Sci, 21 (1998) p.1.